Journal of Alloys and Compounds 506 (2010) 188–193

Contents lists available at ScienceDirect

Journal of Alloys and Compounds

journal homepage: www.elsevier.com/locate/jallcom

# Electrical characterization of nanocluster n-CdO/p-Si heterojunction diode

Fahrettin Yakuphanoglu[a,*], Mujdat Caglar[b], Yasemin Caglar[b], Saliha Ilican[b]

[a] Firat University, Faculty of Science, Department of Physics, 23169 Elazig, Turkey
[b] Anadolu University, Faculty of Science, Department of Physics, 26470 Eskisehir, Turkey

ARTICLE INFO

*Article history:*
Received 19 February 2010
Received in revised form 22 June 2010
Accepted 30 June 2010
Available online 8 July 2010

*PACS:*
73.63.Bd
61.46.−w
77.84.Bw
73.40.Kp

*Keywords:*
Nanostructures
Nanomaterials
Oxides
Heterojunction semiconductor devices

ABSTRACT

The nanocluster n-CdO/p-Si heterojunction diode was fabricated by sol–gel method. The structural and optical properties of the nanocluster CdO film have been investigated. The CdO film has a polycrystalline with a cubic monteponite phase. The scanning electron microscopy images indicate that the surface morphology CdO film is almost homogeneous and the CdO film is consisted of the clusters formed with coming together of the nanoparticles. The optical band gap of the CdO film was found to be 2.45 eV using optical absorption method. The electrical properties of the p–n heterojunction composed of transparent CdO and p-Si semiconductors were investigated by current–voltage and conductance–frequency methods. The ideality factor of the diode was found to be 5.41 and the obtained $n$ value is higher than unity due to the interface states between the two semiconductor materials and series resistance. The reverse current of the diode strongly increases with illumination intensity of 100 mW cm$^{-2}$ and the diode gives a maximum open circuit voltage $V_{oc}$ of 0.12 V and short-circuits current $I_{sc}$ of $0.53 \times 10^{-6}$ A. The interface state density values for the diode were found to vary from $7.82 \times 10^{13}$ to $3.02 \times 10^{12}$ eV$^{-1}$ cm$^{-2}$ under various bias voltages.

© 2010 Elsevier B.V. All rights reserved.

## 1. Introduction

In recent years, metal-oxide films such as ZnO, CdO, $SnO_2$, $TiO_2$, etc. that are both transparent in the visible region and electrically conducting have been extensively investigated due to their potential applications in displays, phototransistors [1–3], photovoltaic solar cells [4], gas sensors [5], and other optoelectronic devices [6]. For most optoelectronic devices such as flat panel displays, it is essential to use a transparent electrode consisting of a transparent conductive oxide (TCO) semiconductor. All the TCO films have n-type conductivity. The high conductivity of these films results mainly from stoichiometric deviation. The conduction electrons in these films are supplied from donor sites associated with oxygen vacancies or excess metal ions.

TCOs are essential part of electronic technology, which require both large-area electrical contact and optical access in the visible portion of the light spectrum. High transparency combined with useful electrical conductivity is achieved by selecting a wide-band gap oxide. CdO is a one of TCOs and it has a relatively low intrinsic band gap of 2.3 eV [7]. Despite of its low band gap, it can reach a high band gap value owing to its low effective carrier mass [8], giving rise to relatively large shifts due to doping.

There are several methods developed on synthesis of CdO films such as spray pyrolysis [9], sputtering [10], chemical bath deposition (CBD) [11], pulsed laser deposition [12,13], and MOCVD [14,15]. However, there are a few reports on the synthesis of them using a sol–gel spin coating method [16–20]. The sol–gel spin coating method has various advantages such as cost effectiveness, thin, transparent, multicomponent oxide layers of many compositions on various substrates, simplicity, excellent compositional control, homogeneity and lower crystallization temperature.

There exists a strong technological trend to use nanometer scale structures in semiconductor electronics. In nanoscale, dimensional confinement and the surface effect is substantially greater than in the bulk, which will result in a better optical properties and enhanced electrical properties in device. However, assembling nanostructures into devices is still challenging due to the difficulties in manipulating structures of such small size. In an earlier paper [21], we have reported the electrical properties of flower-like CdO/p-Si heterojunction diode in the temperature range of 80–400 K. The CdO film deposited on p-Si had a flower-like structure. It was seen that the charge transport mechanism of the diode changed from the tunneling mechanism to the recombination mechanism, when the temperature was varied from lower temperatures to higher temperatures. In the present work, the solution preparation conditions of CdO film production which was used in our previous study were changed and the CdO film with nanoclusters formed with the coming together

* Corresponding author. Tel.: +90 424 2370000 3621; fax: +90 424 2330062.
*E-mail address:* fyhanoglu@firat.edu.tr (F. Yakuphanoglu).

0925-8388/$ – see front matter © 2010 Elsevier B.V. All rights reserved.
doi:10.1016/j.jallcom.2010.06.174

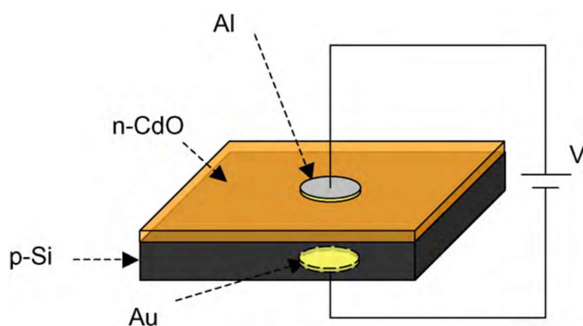


**Fig. 1.** The schematic structure of nanocluster n-CdO/p-Si heterojunction diode.

of the nanoparticles was grown on p-Si(1 0 0). The nanocluster n-CdO/p-Si heterojunction diode was fabricated and the electrical properties of the diode were analyzed by current–voltage and capacitance–conductance–voltage techniques at room temperature.

## 2. Experimental

In this work, the sol–gel spin coating method was used to deposit the CdO film. The coating solution was prepared by using 0.5 M cadmium acetate dihydrate [$C_4H_6CdO_4{\cdot}2H_2O$] together with 2-methoxethanol and monoethanolamine (MEA). 2-methoxethanol and MEA were a solvent and stabilizer, respectively. The molar ratio of MEA to cadmium acetate dihydrate was maintained at 1:1. The solution was stirred constantly during its preparation. The procedure was done entirely at room temperature. The solution was stirred at room temperature for 2 h to yield a clear and homogeneous solution. The coating solution was dropped onto silicon and then the silicon was rotated at 3000 rpm. After the spin coating, the film was dried at 300 °C for 10 min. This coating/drying procedure was repeated for ten times and then annealed at 450 °C in air for 1 h. A CdO film was also deposited on a cleaned indium tin oxide (ITO) coated conducting glass substrate at the same experimental conditions by the sol–gel spin coating method. Thus, the CdO films which were deposited both on the p-Si and ITO were fabricated at the same time and conditions. The substrate used for the fabrication of n-CdO/p-Si heterojunction diode is a p-type (boron-doped) single crystal silicon ⟨1 0 0⟩ with a thickness of 600 μm and a resistivity of 1–10 Ω-cm. First, Si wafer was degreased through RCA cleaning procedure, i.e., a 10 min boiling in $NH_4OH + H_2O_2 + 6$ deionized (DI) (18 MΩ DI water), which was followed by a 10 min boiling in $HCl + H_2O_2 + 6$ DI. Before forming an CdO layer on p-type Si substrate, the native oxide on the polish surface of the substrate was removed in HF:$H_2O$ (1:10) solution, and finally, the wafer was rinsed in DI water. The CdO film was deposited on silicon by sol–gel spin coating method. For the electrical measurements of n-CdO/p-Si heterojunction diode, the metal electrodes were formed both back surface of the Si wafer and top of the CdO film. Fig. 1 shows the schematic diagram of an n-CdO/p-Si heterojunction diode.

The crystal structure of the film was investigated using RIGAKU 2200 X-ray diffraction (XRD) system with a CuKα source. Surface morphology and elemental analysis were studied using a ZEISS SUPRA 50VP model scanning electron microscope (SEM) and BRUKER AXS energy dispersive X-ray spectroscopy (EDX), respectively. The CdO film deposited on the ITO substrate was only used for the optical properties. The absorbance of the CdO film deposited on the ITO substrate was measured in the spectral region of 190–900 nm using a Shimadzu UV 2450 spectrophotometer with an attached integrating sphere at room temperature. The thickness of the CdO film was determined with Mettler Toledo MX5 microbalance by using weighing method. It was found to be 573 nm. The current–voltage and capacitance–voltage characteristics of the diode were performed using a KEITHLEY 4200 SCS/CVU semiconductor characterization system. The photocurrent measurements were performed using a white light source under 100 mW cm$^{-2}$ intensity by a KEITHLEY 6517A Electrometer.

## 3. Results and discussion

### 3.1. The structural and morphological properties of the CdO film

Fig. 2 shows an XRD spectrum of polycrystalline CdO film grown on silicon. All the peaks belong to cubic monteponite phase of the CdO (JCPDS card no: 05-0640). The texture coefficient (*TC*) represents the texture of particular plane, deviation of which from unity implies the preferred growth. Quantitative information concerning the preferential crystallite orientation was obtained from the different texture coefficient $TC(h\,k\,l)$ expressed by [22]

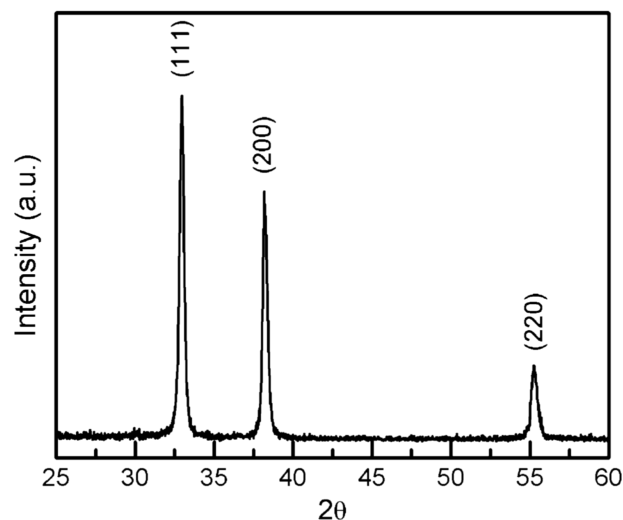


**Fig. 2.** XRD pattern of the CdO film.

$$TC(h\,k\,l) = \frac{I(h\,k\,l)/I_o(h\,k\,l)}{N^{-1}\sum_n I(h\,k\,l)/I_o(h\,k\,l)} \quad (1)$$

where $I(h\,k\,l)$ is the measured relative intensity of a plane $(h\,k\,l)$, $I_o(h\,k\,l)$ is the standard intensity of the plane $(h\,k\,l)$ taken from the JCPDS data, $N$ is the reflection number and $n$ is the number of diffraction peaks. A sample with randomly oriented crystallite presents $TC(h\,k\,l) = 1$, while the larger value, the larger abundance of crystallites oriented at the $(h\,k\,l)$ direction. The texture coefficients were calculated for all the peaks. $I(h\,k\,l)/I_o(h\,k\,l)$ and $TC(h\,k\,l)$ values were found to be 1.54, 1.13 and 0.33 for planes (1 1 1), (2 0 0) and (2 2 0), respectively. So, the CdO film is polycrystalline with the preferential orientation along the (1 1 1) crystal plane, and this agrees well with the structure of CdO film prepared by the same method [4,18–21,23]. The average crystallite size of CdO film was calculated using the well known Scherrer's equation [24]. The average crystallite size for the CdO film was found to be 26 nm for the (1 1 1) plane. No metallic cadmium phases were observed in the XRD pattern.

Fig. 3a and b shows the SEM images of the CdO film which were used on the nanocluster n-CdO/p-Si structure at two different magnifications. In Fig. 3a, the clusters which homogenously spread on the whole of the film surface are seen. Also, as seen in Fig. 3b, the clusters are formed from the nanoparticles. The sizes of the clusters are approximately 300–500 nm and the diameters of nanoparticles are about 30–40 nm.

The EDX spectrum of the CdO film is presented in Fig. 4. Only Si, Cd and O signals were detected. The Si element that is not expected to be in solid film may probably result from the Si substrate. So, EDX results confirm the chemical structure of the CdO.

### 3.2. The optical band gap of the CdO film

The following relation [25] was used to calculate the optical band gap with direct transitions of the CdO film,

$$(\alpha h\nu) = B(h\nu - E_g)^{1/2} \quad (2)$$

where $h\nu$ is the photon energy, $\alpha$ is the absorption coefficient, $E_g$ is the optical band gap and $B$ is a constant. For calculation of the optical band gap of CdO film, the curve of $(\alpha h\nu)^2$ vs. $h\nu$ was plotted. The $E_g$ value of the CdO film was determined from Fig. 5 and it was found to be 2.45 eV. This value is in agreement with the known range of values (2.2–2.6 eV) for the CdO [16,19–21]. Bulk CdO is a semicon-

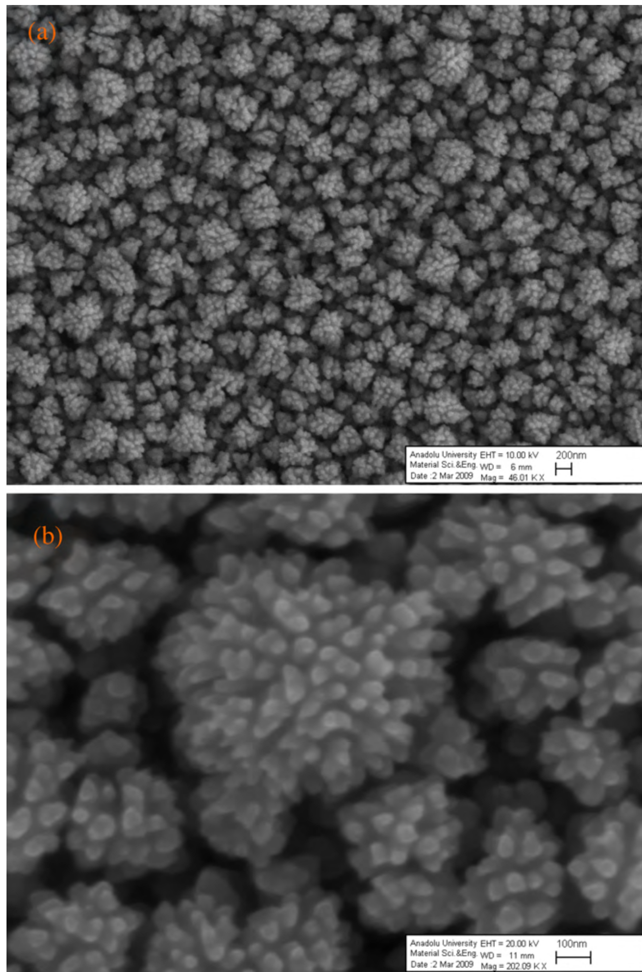


**Fig. 3.** SEM image of the nanocluster CdO film under 46,000 (a) and 202,000 (b) magnifications.

ductor with one direct band gap of 2.3 eV and one indirect gaps of 1.36 eV [26,27]. The obtained band gap value is larger than the bulk value. If the crystallite size decreases, the band gap energy should increase. As a similar result was also reported by Vigil et al. [28]. They reported that the optical band gap value of CdO was 2.53 eV and the particle size of this film was 18 nm. Also, they observed a decrease of the band gap energy when the diameter of CdO crystallites becomes larger. We found the average crystallite size as 26 nm. So, the results are in agreement with each other.

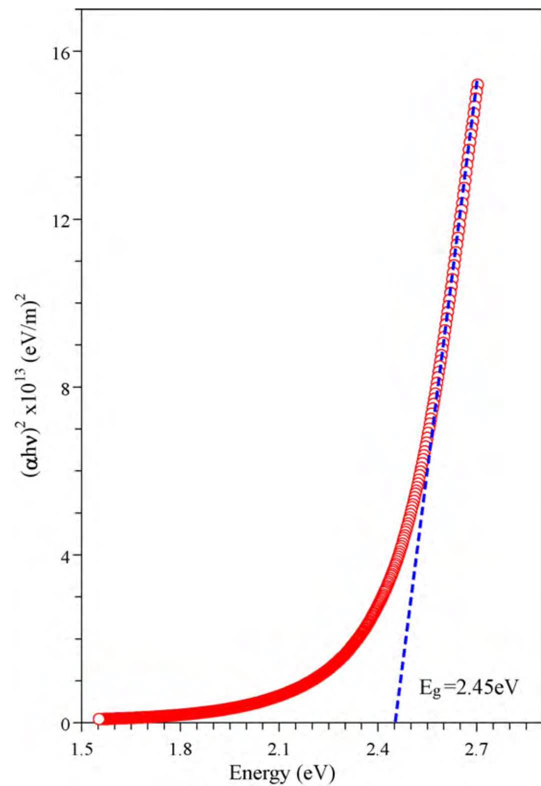


**Fig. 5.** The plot of $(\alpha h\nu)^2$ vs. $h\nu$ of the nanocluster CdO film.

### 3.3. The current–voltage characteristics of the nanocluster n-CdO/p-Si heterojunction diode

The current–voltage ($I$–$V$) characteristics of the nanocluster n-CdO/p-Si heterojunction diode are shown in Fig. 6. As seen in Fig. 6, the diode indicates a rectifying contact between n-CdO and p-Si semiconductors and the rectifying ratio of the diode is 37 at ±2 V. The $I$–$V$ characteristics of the diode can be analyzed by the following relation [29],

$$I = I_o\left[\exp\left(\frac{qV}{nkT}\right) - 1\right] \quad (3)$$

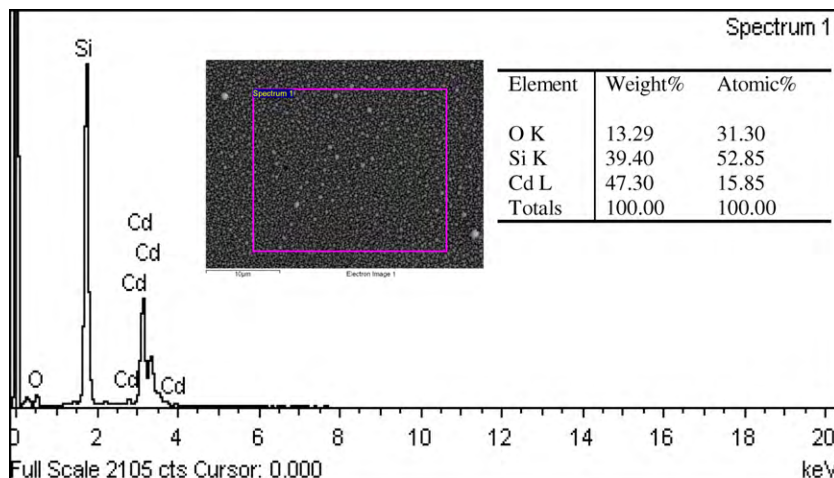


| Element | Weight% | Atomic% |
|---|---|---|
| O K | 13.29 | 31.30 |
| Si K | 39.40 | 52.85 |
| Cd L | 47.30 | 15.85 |
| Totals | 100.00 | 100.00 |

**Fig. 4.** Elemental analysis of the nanocluster CdO film and SEM image of the region analyzed (inset image).

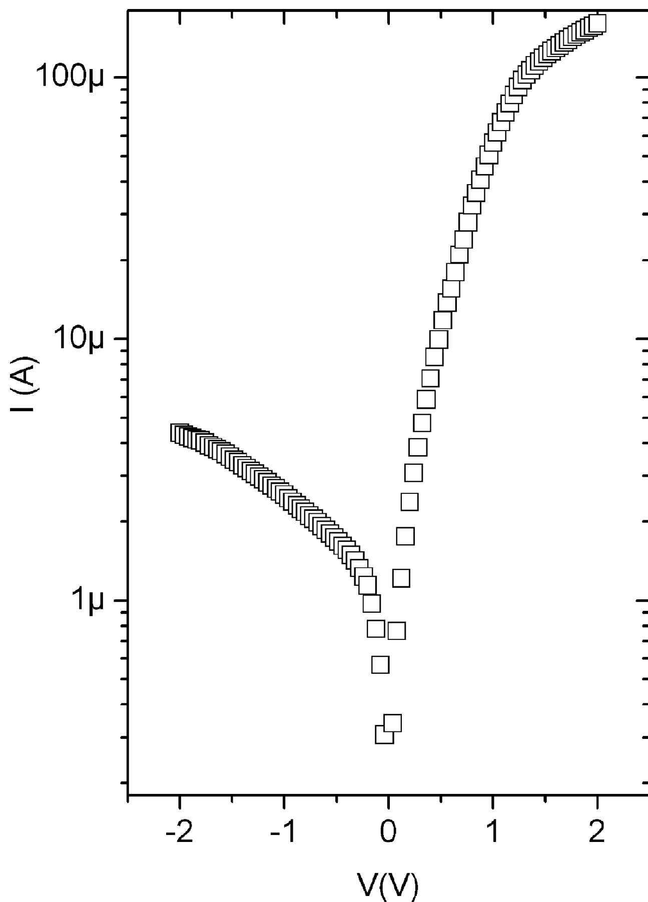


**Fig. 6.** Current–voltage characteristics of the nanocluster n-CdO/p-Si heterojunction diode.

where $V$ is the applied voltage, $n$ is the ideality factor, $k$ is the Boltzmann constant, $T$ is the temperature and $I_o$ is the reverse saturation current. The ideality factor of the diode was determined from the slope of the linear region of forward bias of Fig. 6 and it was found to be 5.41. The obtained $n$ value is higher than unity due to the interface states and series resistance. The obtained $n$ value suggests that the charge transport mechanism is controlled by recombination in the space charge region.

Having a high performance of a diode depends on the high crystalline quality of the semiconductor, low surface-state density and ideal ohmic and Schottky contacts being made. Thus, as the crystallite size decreases, the surface plays an increasingly important role on the device performance. The surface has to be homogeneous and free from the defects.

In order to determine the series resistance and the barrier height of the diode, we used Norde method given by the following relation [30],

$$F(V) = \frac{V_0}{\gamma} - \frac{kT}{q}\left(\frac{I(V)}{A^*AT^2}\right) \quad (4)$$

where $\gamma$ is the integer (dimensionless) greater than $n$. $I(V)$ is the current obtained from the $I$–$V$ characteristic. Fig. 7 shows the plot of $F(V)$ vs. voltage for the diode. In Norde model, the barrier height is defined as follows,

$$\Phi_b = F(V_0) + \frac{V_0}{\gamma} - \frac{kT}{q} \quad (5)$$

where $F(V_o)$ is the minimum point of $F(V)$. The barrier height was found to be 0.56 eV. The series resistance is given by the following relation

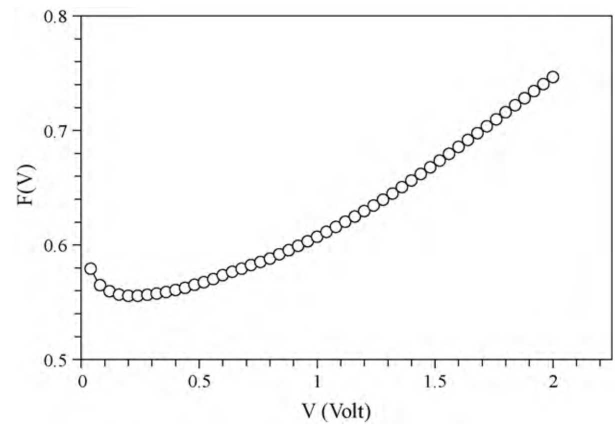


**Fig. 7.** Plot of $F(V)$ vs. $V$ for the nanocluster n-CdO/p-Si heterojunction diode.

$$R_s = \frac{kT(\gamma - n)}{qI_1} \quad (6)$$

where $\gamma$ is the integer (dimensionless) greater than $n$, $q$ is the charge of an electron and $I_1$ is the current obtained from the minimum point of $F(V)$. The $R_s$ value for the diode was determined using Eq. (6) and was found to be 6.41 kΩ. The obtained $R_s$ value is considerable high due to CdO and oxide layers and this causes a non-linear behavior.

In order to characterize the photovoltaic behavior of the diode, the $I$–$V$ characteristics of the diode under dark and illumination conditions were performed, as shown in Fig. 8. As seen in Fig. 8, the reverse current strongly increases with illumination intensity of 100 mW cm$^{-2}$ and the diode gives a maximum open circuit voltage $V_{oc}$ of 0.12 V and short-circuits current $I_{sc}$ of $0.53 \times 10^{-6}$ A. These values indicate that the n-CdO/p-Si diode exhibits a photovoltaic behavior, because the photovoltaic effect involves the creation of a voltage and current in a p–n heterojunction upon exposure to light intensity. The open circuit voltage $V_{oc}$ of the n-CdO/p-Si diode is low. Thus, this device can be used as a photodiode rather than solar cell in optoelectronic devices applications and furthermore, the photodiodes are routinely designed to achieve a spectral response or a rapid time response [31].

The phototransient current plot of the diode is shown in Fig. 9. As seen in Fig. 9, the photocurrent changes with time after turning on and off situations. The diode exhibits good photoconductivity. After the switching light on the diode, the photocurrent indicates an abrupt increase and in short time, the photocurrent shows a stable plateau value. This increase in the photocurrent of the diode depends on the difference between the electron affinities of the p-Si and CdO semiconductors. After the light off switching, the current reaches the first situation.

### 3.4. *The band structure of the nanocluster n-CdO/p-Si heterojunction diode*

The band structure of nanocluster n-CdO/p-Si heterojunction diode can be constructed using Anderson model [32]. In the construction of the band structure, the effect of interfacial state is neglected. The presence of an ultrathin silicon oxides layer that may occur between the CdO film and silicon substrate is neglected. So, its effect on the energy band structure is also neglected. Fig. 10 shows the constructed band structure of the n-CdO/p-Si heterojunction diode under forward bias. In this diagram, the values of band gaps of $E_g$(CdO) = 2.45 eV and $E_g$(Si) = 1.12 eV, the electron affinity for CdO, $\chi$(CdO) = 4.51 eV and the electron affinity for Si $\chi$(Si) = 4.05 eV were used. As shown in Fig. 10, the conduction-band

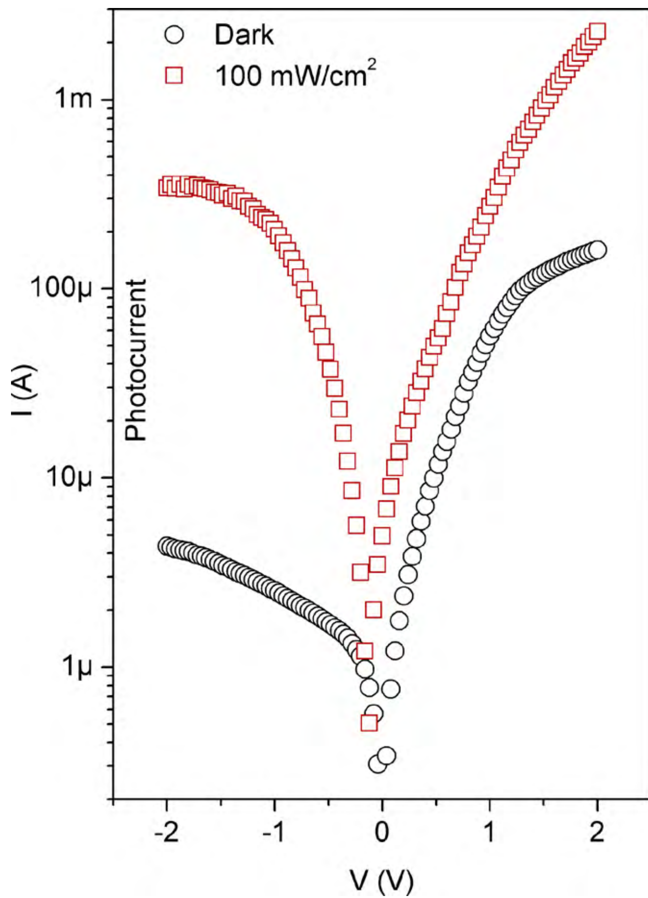


**Fig. 8.** Current–voltage characteristics of the nanocluster n-CdO/p-Si heterojunction diode under dark and illumination conditions.

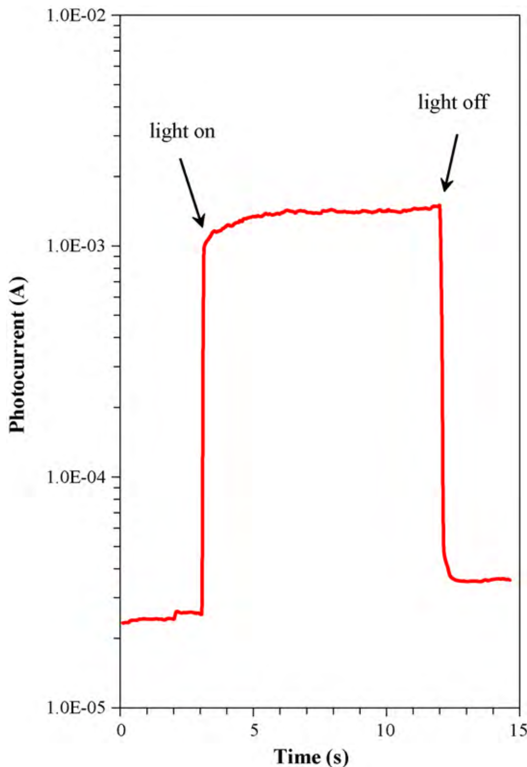


**Fig. 9.** Time dependent photocurrent response of the nanocluster n-CdO/p-Si heterojunction diode under 100 mW cm$^{-2}$ illumination.

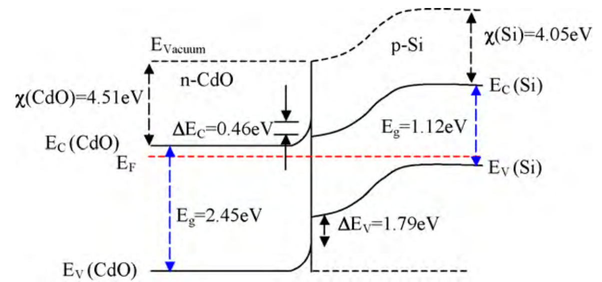


**Fig. 10.** The band structure of the nanocluster n-CdO/p-Si heterojunction diode under forward bias.

offset is $\Delta E_C = \chi(\text{CdO}) - \chi(\text{Si}) = 0.46$ eV, and the valance-band offset $\Delta E_V = E_g(\text{CdO}) - E_g(\text{Si}) + \Delta E_C = 1.79$ eV. $\Delta E_V$ has a higher value the $\Delta E_C$. This means that, the injection of electrons from n-CdO to p-Si is greater than the hole injection from p-Si to n-CdO. Under forward bias, electrons can be easily injected into the p-Si side because of the small potential barrier. Thereby the forward current rapidly increases under a higher voltage bias.

### 3.5. *The capacitance–voltage characteristics of the nanocluster n-CdO/p-Si heterojunction diode*

Fig. 11 shows the plot of $1/C^2$ vs. $V$ of nanocluster n-CdO/p-Si heterojunction diode. The capacitance increases with the bias voltage and reaches a constant value. As seen in Fig. 11, the plot of $1/C^2$ vs. $V$ deviates from the linearity. This non-linear behavior is attributed to the more electronic states and expanding of the depletion region width. This non-linearity of the $1/C^2$ vs. $V$ curve is in agreement with the poor *I–V* characteristics of the diode.

For the determination of the interface state density of the diode, we used the admittance spectroscopy. The admittance for studied diode can be expressed by the following relation

$$Y = G_m + i\omega C_m \tag{7}$$

where $G_m$ and $C_m$ are the measured conductance and capacitance values, respectively.

The conductance of the interface states can be expressed as [33],

$$\frac{G_{it}}{\omega} = \frac{\omega G_m C_{ox}^2}{G_m^2 + \omega^2 (C_{ox} - C_m)^2} \tag{8}$$

where $G_{it}$ is the conductance of the interface states, $C_{ox}$ is the capacitance of oxide layer. The interface conductance for the diode is

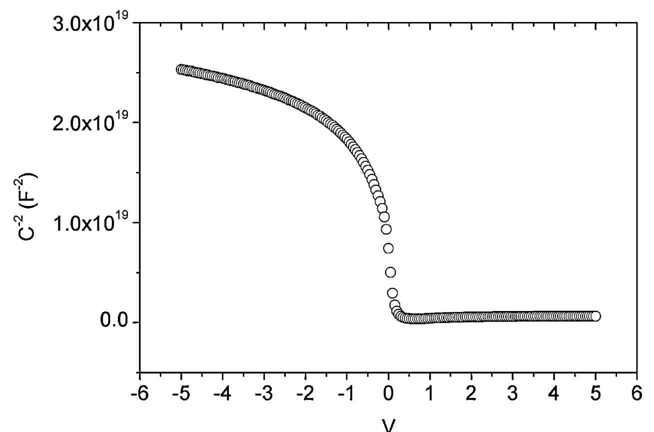


**Fig. 11.** Capacitance–voltage characteristics of the nanocluster n-CdO/p-Si heterojunction diode under 500 kHz.

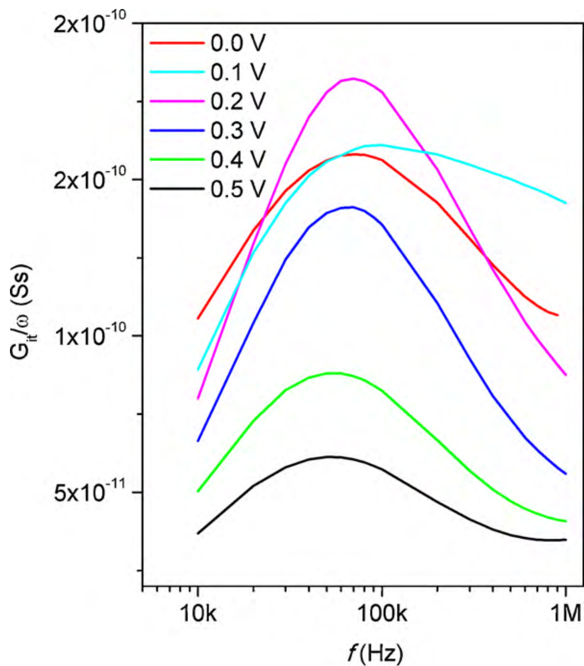


**Fig. 12.** Plots of $G_{it}/\omega$ vs. frequency of the nanocluster n-CdO/p-Si heterojunction diode under various voltages.

expressed as follows [33],

$$\frac{G_{it}}{\omega} = \frac{q\omega\tau_{it}D_{it}}{1+(\omega\tau_{it})^2} \tag{9}$$

where $D_{it}$ is density of the interface states, $q$ is the charge of an electron, $\omega$ is the angular frequency, $\tau_{it}$ is the time constant of the interface states. The plots of $(G_{it}/\omega)$ vs. log$f$ of the diode under various bias voltages are shown in Fig. 12. The plots of $(G_{it}/\omega)$ vs. log$f$ show peaks and the position of the peaks shifts to the lower frequencies with applied voltages. The interface state density of the diode was determined from Fig. 12 using the relation

$$D_{it} = \frac{(G_{it}/\omega)_{\max}}{0.402qA} \tag{10}$$

where A is the diode contact area. The $D_{it}$ values for the diode vary from $7.82 \times 10^{13}$ to $3.02 \times 10^{12}$ eV$^{-1}$ cm$^{-2}$, when the applied voltage changes from 0 to 0.5 V. The $D_{it}$ values decrease with increasing bias voltages. The value of $3.02 \times 10^{12}$ eV$^{-1}$ cm$^{-2}$ is considered 'high' for the fabrication of n-CdO/p-Si heterojunction diode with high performance. It is evaluated that the role of nanoclusters in transport phenomena as nanoparticles will introduce the energy levels in band gap of the material and results in the increase the interface state density at the interface. For device with high performance, it is need to be reduced and further work is required in order to achieve values as low as $10^{10}$ eV$^{-1}$ cm$^{-2}$.

## 4. Conclusions

The nanocluster n-CdO/p-Si heterojunction diode was fabricated by sol–gel spin coating method. The structural and optical properties of the CdO film were investigated. As a result of these characterizations, it was observed that the CdO film had a polycrystalline with a cubic monteponite phase and its optical band gap was 2.45 eV. The SEM images indicated that the surface of the CdO film consists of the clusters formed with the coming together of the nanoparticles. The nanocluster n-CdO/p-Si heterojunction diode exhibited a non-ideal behavior with ideality factor of 5.41 and a photovoltaic behavior under illumination. The obtained results show that the nanocluster n-CdO/p-Si heterojunction diode can be used for the sensor and optoelectronic applications. The high ideality factor of nanocluster n-CdO/p-Si heterojunction diode is not fully understood, although such high value can be commonly attributed to the interface states and series resistance. So, we will effort to improve the quality of this device.

## Acknowledgement

This work was supported by Anadolu University Commission of Scientific Research Projects under grant no. 061039.

## References


[1] N. Ito, Y. Sato, P.K. Song, A. Kaijio, K. Inoue, Y. Shigesato, Thin Solid Films 496 (2006) 99.
[2] J.T. Lim, C.H. Jeong, A. Vozny, J.H. Lee, M.S. Kim, G.Y. Yeom, Surf. Coat. Technol. 201 (2007) 5358.
[3] R. Navamathavan, C.K. Choi, S.J. Park, J. Alloys Compd. 475 (2009) 889.
[4] S. Ilican, Y. Caglar, M. Caglar, M. Kundakci, A. Ates, Int. J. Hydrogen Energy 34 (2009) 5201.
[5] M.C. Carotta, V. Guidi, G. Martinelli, M. Nagliati, D. Puzzovio, D. Vecchi, Sens. Actuators B: Chem. 130 (2008) 497.
[6] S. Goldsmith, Surf. Coat. Technol. 201 (2006) 3993.
[7] R.J. Deokate, S.V. Salunkhe, G.L. Agawane, B.S. Pawar, S.M. Pawar, K.Y. Rajpure, A.V. Moholkar, J.H. Kim, J. Alloys Compd. 496 (2010) 357.
[8] S. Jin, Y. Yang, J.E. Medvedeva, L. Wang, S. Li, N. Cortes, J.R. Ireland, A.W. Metz, J. Ni, M.C. Hersam, A.J. Freeman, T.J. Marks, Chem. Mater. 20 (2008) 220.
[9] P.M. Devshette, N.G. Deshpande, G.K. Bichile, J. Alloys Compd. 463 (2008) 576.
[10] Q. Zhou, Z. Ji, B. Hu, C. Chen, L. Zhao, C. Wang, Mater. Lett. 61 (2007) 531.
[11] M. Ortega, G. Santana, A. M-Acevedo, Solid State Electron. 44 (2000) 1765.
[12] B.J. Zheng, J.S. Lian, L. Zhao, Q. Jiang, Appl. Surf. Sci. 256 (2010) 2910.
[13] R.K. Gupta, K. Ghosh, R. Patel, S.R. Mishra, P.K. Kahol, Mater. Lett. 62 (2008) 4103.
[14] Z. Zhao, D.L. Morel, C.S. Ferekides, Thin Solid Films 413 (2002) 203.
[15] D. Lamb, S.J.C. Irvine, Thin Solid Films 518 (2009) 1222.
[16] J. Santos-Cruz, G. Torres-Delgado, R. Castanedo-Perez, S. Jiménez-Sandoval, O. Jiménez-Sandoval, C.I. Zúñiga-Romero, J. Márquez Marín, O. Zelaya-Angel, Thin Solid Films 493 (2005) 83.
[17] K.R. Murali, A. Kalaivanan, S. Perumal, N.N. Pillai, J. Alloys Compd. (2009), doi:10.1016/j.jallcom.2009.11.187.
[18] S Aksoy, Y. Caglar, S. Ilican, M. Caglar, Int. J. Hydrogen Energy 34 (2009) 5191.
[19] S. Ilican, M. Caglar, Y. Caglar, F. Yakuphanoglu, Optoelectron. Adv. Mater. 3 (2009) 135.
[20] Y. Caglar, M. Caglar, S. Ilican, A. Ates, J. Phys. D: Appl. Phys. 42 (2009) 065421.
[21] M. Caglar, F. Yakuphanoglu, J. Phys. D: App. Phys. 42 (2009) 045102.
[22] C.S. Barret, T.B. Massalski, Structure of Metals, Pergamon Press, Oxford, 1980.
[23] A.A. Dakhel, A.Y. Ali-Mohamed, Mater. Chem. Phys. 113 (2009) 356.
[24] B.D. Cullity, S.R. Stock, Elements of X-Ray Diffraction, 3rd ed., Prentice Hall, 2001.
[25] J.I. Pankove, Optical Processes in Semiconductors, Prentice Hall Inc., Englewoord Cliffs, NJ, 1971.
[26] K. Gurumurugan, D. Mangalaraj, Sa.K. Narayandass, J. Cryst. Growth 147 (1995) 355.
[27] N. Ueda, H. Maeda, H. Hosono, H. Kawazoe, J. Appl. Phys. 84 (1998) 6174.
[28] O. Vigil, F. Cruz, A.M. Acevedo, G.C. Puente, L. Vaillant, G. Santana, Mater. Chem. Phys. 68 (2001) 249.
[29] S.M. Sze, Physics of Semiconductor Devices, 2nd ed., Wiley, New York, 1981.
[30] H. Norde, J. Appl. Phys. 50 (1979) 5052.
[31] F. Yakuphanoglu, Sens. Actuators A 141 (2008) 383.
[32] G. Milnes, D.L. Feucht, Heterojunctions and Metal-Semiconductor Junctions, Academic, New York, 1972.
[33] E.H. Nicollian, J.R. Brews, MOS (Metal Oxide Semiconductor) Physics and Technology, Wiley, New York, 1982.